Thermodynamic evolution of phase explosion during high-power nanosecond laser ablation

Quanming Lu*

School of Earth and Space Sciences, University of Science and Technology of China, Hefei, 230026, China

It is argued that phase explosion plays an important role during high-power laser ablation. A theoretical model which includes the effect of an expanding mass plasma has been developed to describe the process of phase explosion during the interactions of a high-power nanosecond laser pulse on an aluminum target. For a laser with a 3-ns pulse duration, if the laser intensity is high enough ($\geqslant 5 \times 10^{10}$ W/cm^2), phase explosion was found to occur after the completion of the laser pulse, but not during the process of laser energy deposition. This result is consistent with recent experiments. It is also found that the pressure of the induced ablation plasma plays a crucial role in the process of phase explosion.

Laser ablation is a process whereby materials are removed from the surface of a solid by laser irradiation. It is finding applications in a growing number of areas, such as deposition of metal and dielectric films and laser ablation chemical analysis [1]. Laser ablation is also of great interest from a basic physical point of view. Its fundamental mechanisms are not fully understood, especially when high-power laser pulses are utilized and superheating of the target material occurs. Miotello and Kelly suggested that when the laser irradiance is sufficiently high so that the target surface reaches a temperature $\sim 0.9 T_C$ (T_C is the thermodynamic critical temperature), phase explosion might be a mechanism that removes materials from the laser-ablated target [2,3]. In this process, homogeneous bubble nucleation occurs, and the target makes a rapid transition from a superheated liquid layer to a mixture of vapor and liquid droplets, which then eject from the target surface. These authors suggested that for high-power nanosecond laser pulse, phase explosion occurs during the laser pulse. However, recently experimental results using a Nd:YAG laser pulse with a 3-ns pulse duration on a silicon target revealed that phase explosion would occur after the completion of the laser pulse [4,5].

The theory of phase explosion may be considered from either a kinetic or a thermodynamic viewpoint. The former models the rate and the probability of vapor bubble formation at any temperature, while the latter provides a rigorous method by which to predict the limit of superheated liquid [6]. According to kinetic theory, when the liquid is superheated, homogeneous bubble nucleation occurs. If these bubbles reach a critical radius r_c, they will grow spontaneously. Bubbles with a radius less than r_c are likely to collapse. When the radii of a definite number of bubbles are larger than r_c, phase explosion will happen [7,8]. Based on this kinetic theory, Lu *et al.* demonstrated that phase explosion can occur after the completion of the laser pulse provided the pulse is sufficiently short ($<$tens of ns) [9]. While various models have been developed to study the phase explosion during ultrafast laser ablation [10], relatively little attention has been paid to mechanisms of phase explosion for high-power nanosecond laser pulse. In this paper, using a

one-dimensional fluid model we calculate the thermodynamic process of phase explosion during nanosecond laser ablation of an Al target. The model results are consistent with those from the kinetic theory as well as the experimental results, which indicate that phase explosion occurs after completion of the laser pulse.

Since its thermal and optical properties are well characterized, aluminum is selected as the target material [11–13]. The ablation laser pulse for the simulation is a 532-nm-wavelength Gaussian beam with 3 ns full width at half maximum (FWHM). Initially, the semi-infinite Al target is set at its melting point, whose mass density and temperature are 2.7 g/cm^2 and 933 K, respectively. According to Ref. [14], we can describe the target material by the generalized van der Waals (GvdW) equations with parameter $\gamma=4.846$. A one-dimensional fluid model has been established to describe phase evolutions of the target during laser ablation, and the fluid equations for the conservation of mass, momentum, and energy are as follows:

$$\frac{\partial \rho}{\partial t} + \frac{\partial}{\partial x}(\rho u) = 0, \tag{1}$$

$$\frac{\partial u}{\partial t} + u\frac{\partial u}{\partial x} = -\frac{1}{\rho}\frac{\partial p}{\partial x}, \tag{2}$$

$$\frac{\partial h}{\partial t} + u\frac{\partial h}{\partial x} = -p\frac{\partial u}{\partial x} + \frac{\partial}{\partial x}\left(k\frac{\partial T}{\partial x}\right) + S, \tag{3}$$

where $h=CT$ is the enthalpy; C is specific heat; ρ, u, T and p are the mass density, velocity, temperature and pressure of the target, respectively; and k is the thermal conductivity. The spatial coordinate x is in the direction normal to the sample surface with origin located at the surface. The source term, S, represents the laser energy absorbed by the target and is expressed as $S=I_{\mathrm{laser}}\alpha \exp(-\alpha x)$. Here, α is the absorption coefficient of the target material at the incident laser wavelength, I_{laser} is the laser irradiance which can reach the target surface. The fluid equations are solved by means of the MacCormack method. After the laser is focused on the surface of the target, the target undergoes vaporization from the extreme outer surface. The vaporization flux is governed by

*FAX: +86-551-3607615. Email address: qmlu@ustc.edu.cn

the Hertz-Knudsen equations, and the velocity of the surface recession can be calculated as [2]

$$\left.\frac{\partial x}{\partial t}\right|_{x=0} = \beta p_b \frac{m}{\rho} (2\pi m k_B T)^{-1/2} \exp\left[\frac{L_{ev}m}{k_B}\left(\frac{1}{T_b} - \frac{1}{T}\right)\right].$$

$$(4)$$

Here, β is the vaporization coefficient, p_b is the boiling pressure (normally ~ 0.1 MPa), T_b is the corresponding boiling temperature, k_B is the Boltzmann constant, m is the mass of an Al atom, L_{ev} is the heat of vaporization, ρ and T are mass density and temperature, respectively.

In our model, we also include the absorption of laser-generated vapor plasma from the target surface. Such a plasma has been frequently observed during high-power laser ablations of solids. The laser irradiance at the target surface I_{laser} can be written as $I_{laser} = I_0(t)\exp(-Hk_1)$, where I_0 is the initial laser irradiance and H is the thickness of the plasma. k_1 is the absorption coefficient of the plasma due to the inverse Bremsstrahlung process. In our simulation, we use the model developed by Harrach to describe this plasma process [15].

The energy incident on the surface of the target, I_s, is equal to the difference between the laser energy reaching the target surface and the latent heat of evaporation at the surface [4], i.e.,

$$I_s = I_{laser} - \rho L_{ev} \left.\frac{\partial x}{\partial t}\right|_{x=0}.$$

$$(5)$$

The energy loss to the surrounding air can be ignored because the heat flux is negligible compared to the latent heat of the evaporating vapor. Thus, at the surface of the target, a boundary condition $\partial T/\partial x = 0$ is used. The change of the velocity at the target surface is calculated from the pressure of target surface and plasma.

Figure 1(a) shows the mass density profiles as a function of position at different times. The initial peak laser irradiance is 8×10^{10} W/cm^2. Because the laser energy is absorbed by the surface of the target, a high-temperature area is formed around the surface. Then this high-temperature area penetrates the target due to convection and thermal diffusion. Early in the process, the penetration is dominated by convection, and its velocity is comparable to the speed of sound (~ 2 km/s). Later in the process, thermal diffusion is the main effect, and the thermal penetration depth is comparable to $(kt)^{1/2}$. At $t=35$ ns, the thickness of the high-temperature area is about 20 μm. As the high-temperature area penetrates the target, the surface of the target loses energy due to evaporation, and the temperature at the surface decreases slowly after the laser pulse (<2 ns). As a consequence, the maximum temperature point is located in the interior of the target, not on the target surface, and this can be seen in Fig. 1(a). The mass density and temperature profiles at $t=35$ ns are given in Fig. 1(b); it shows that the profile of mass density is the inverse of that of temperature, because in the target high temperature will generate high pressure and push the fluid away. The relationship between mass density and temperature at other time is similar.
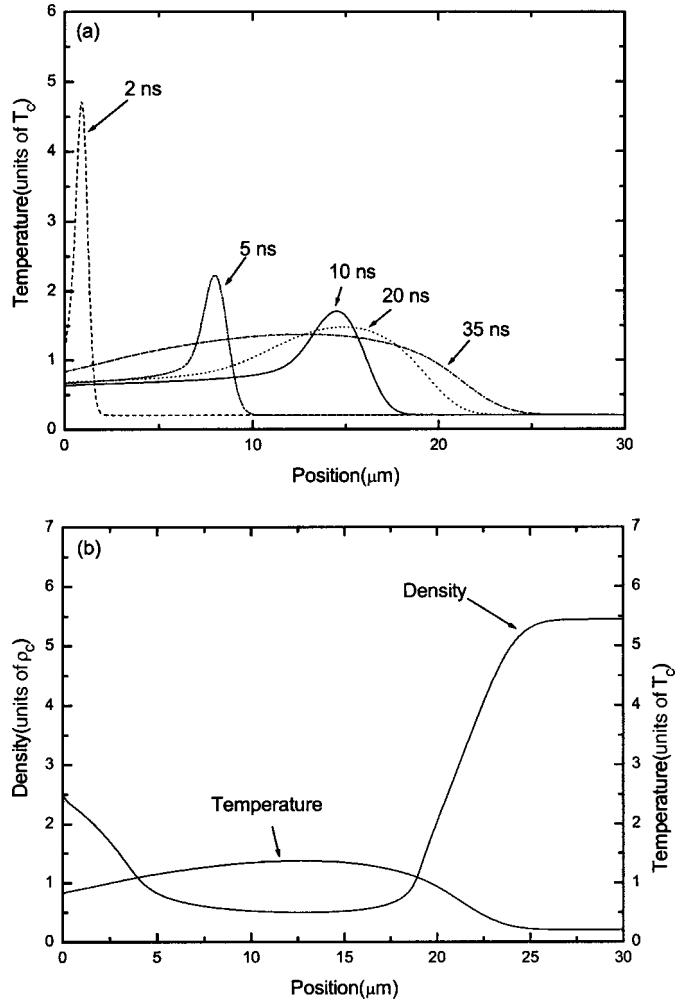
FIG. 1. (a) The mass density profiles as a function of position at different times for peak laser irradiance 8×10^{10} W/cm^2. (b) The mass density and temperature profiles at $t=35$ ns for peak laser irradiance 8×10^{10} W/cm^2.

The evolution of the mass density and temperature of the surface layer is shown in Fig. 2. The peak laser irradiance is 8×10^{10} W/cm^2. In Fig. 2(a), the area enclosed by the spinodal curve (dash-dot line) is marked "Unstable Zone." The spinodal curve is calculated by assuming $(\partial p/\partial \rho)_T = 0$ based on the generalized van der Waals equations. In this unstable zone, the homogeneous matter is unstable due to $(\partial p/\partial \rho)_T < 0$; the least disturbance there will cause the rapid evolution of the thermodynamic state toward one of the two extremes of an isotherm on the spinodal curve, where $(\partial p/\partial \rho)_T = 0$. According to thermodynamics, phase explosion will occur if the phase of the material enters this area. From Fig. 1(b), we know that the most likely area for phase explosion is the target surface, thus we plot the trajectory of the target surface layer in Fig. 2. Figure 2(a) describes the trajectory of the target surface cell in the density-temperature plane, and Fig. 2(b) plots the temporal profiles of the mass density of the target surface layer.

Initially, the mass density and temperature of the surface are $\rho = 5.42\rho_C$ and $T = 0.2045T_C$, respectively (ρ_C and T_C are thermodynamic critical density and temperature of Al).
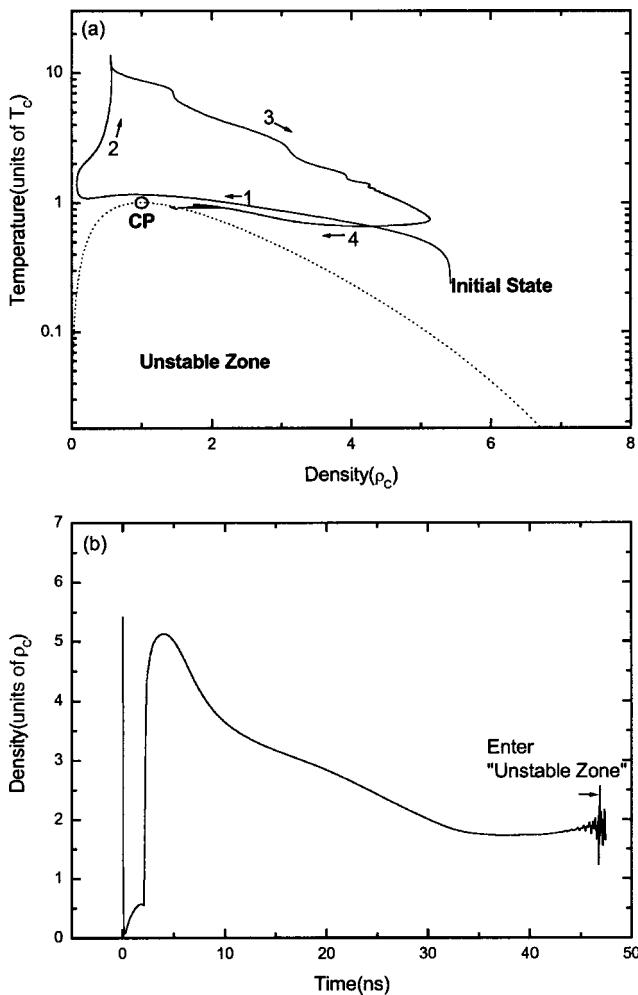
FIG. 2. (a) The phase trajectory of the target surface layer in the density-temperature plane, with the dash-dot curve representing the spinodal line. The value of peak laser irradiance is 8×10^{10} W/cm^2. (b) The temporal profiles of the mass density of the target surface layer.

From Fig. 2, we can find that the evolution of the target surface layer can be divided into four distinctive stages.

(1) During the first stage, the target surface is heated to very high temperature by the laser energy deposition, and the fluid is pushed away due to high pressure, thus an area with small mass density will form near the target surface. If the laser irradiance is higher than a certain threshold, which is about 5×10^{10} W/cm^2, the trajectory of the target surface layer exceeds the critical point (marked a "CP" in the figure); no phase explosion will occur at this stage. From Fig. 2(b), it is easy to find that this stage lasts only about 0.2 ns.

(2) During the second stage, the temperature of the target surface increases rapidly while the mass density is almost constant. The temperature of the target surface can be heated to a very high temperature. This stage lasts about 2 ns. Actually, in this stage, the laser pulse is nearly completed, and the laser-induced plasma is fully developed so that the trailing part of the laser pulse is truncated.

(3) During the third stage, the laser pulse is completed, and no energy is deposited on the target surface. The temperature of the target surface decreases, and the mass density increases. This process will continue about 3 ns.

(4) During the fourth stage, the mass density of the target surface decreases while the temperature remains approximately constant, with its value around $0.9T_C$. It takes about 45 ns for the surface layer to cross the spinodal boundary and enter the unstable zone. Near the spinodal boundary, the mass density shows irregular fluctuations and phase explosion occurs. This result clearly shows that phase explosion does occur after the completion of the laser pulse, which is consistent with the experimental results. The delay time after laser pulse for laser irradiance 8×10^{10} W/cm^2 is about 45 ns.

According to the kinetic theory of phase explosion, after the target is superheated, homogeneous bubble nucleation occurs. It will take the bubbles tens of nanoseconds to grow to critical radius. The target material therefore consists of droplets and vapor bubbles in the unstable zone. The present model lacks this feature to provide an accurate description of the kinetic phenomena. Such a treatment is beyond the scope of a fluid model that deals with macroscopic quantities and treats every part of the matter as a continuous medium. After the phase of the target material enters the unstable zone, it becomes so unstable that our model cannot continue to describe it.

Laser-induced plasma is found to have a profound influence on the details of the phase explosion process. Figure 3 shows the temporal profiles of number densities of electrons and particles (including neutral atoms and ions), electron and particle temperatures, and the plasma pressure (including electrons and particles) for initial peak laser irradiance 8×10^{10} W/cm^2. Initially, the number densities of electrons and particles as well as their corresponding temperatures are very small, and the pressure of the plasma is also very small. The induced plasma is almost transparent to the laser pulse, and most of the laser energy is deposited on the surface of the target, which results in a high temperature at the target surface. The pressure of the target surface is higher than that of the plasma, thus the fluid is pushed away from the target surface, and the mass density of the target surface decreases. This corresponds to the first stage as described above. During the second stage, the target surface continues to be heated, with high-temperature vapor ejected from the target. The number density and temperature of the plasma increase rapidly until the pressure of the plasma is almost the same as that of the target surface. The target surface is heated while its mass density remains a constant.

When the temperature of the electrons and particles as well as their number densities are high enough, plasma breakdown (ionization) occurs. The number density and temperature of the electrons increase dramatically. Eventually, most of the neutral atoms will be ionized. The higher the number density and temperature of the electrons, the more energy is absorbed by the plasma with inverse Bremsstrahlung process until most of the laser energy is absorbed. Thus
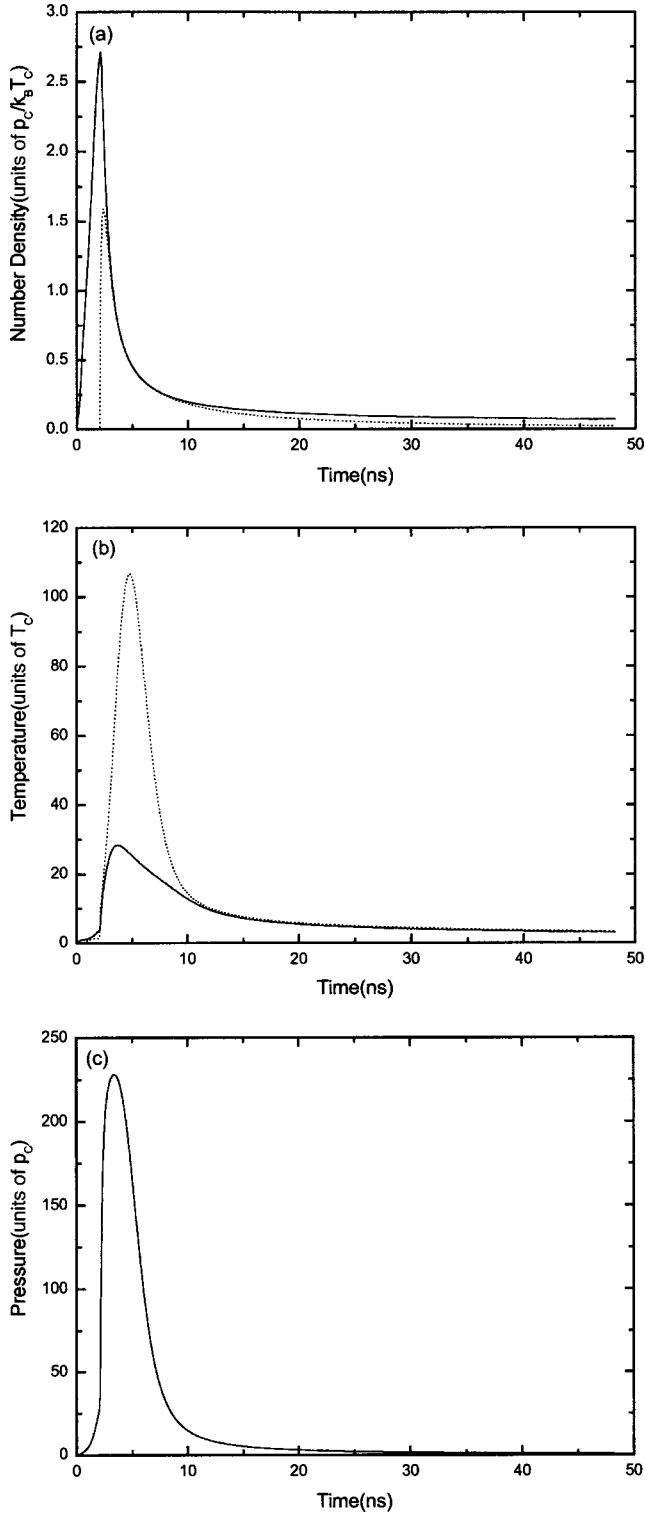
FIG. 3. (a) The temporal profiles of the number densities of electrons and particles for laser irradiance 8×10^{10} W/cm^2. Solid line: particles. Dotted line: electrons. (b) The temporal profiles of electron and particle temperatures for laser irradiance 8×10^{10} W/cm^2. Solid line: particles. Dotted line: electrons. (c) The temporal profile of the plasma pressure for laser irradiance 8×10^{10} W/cm^2.
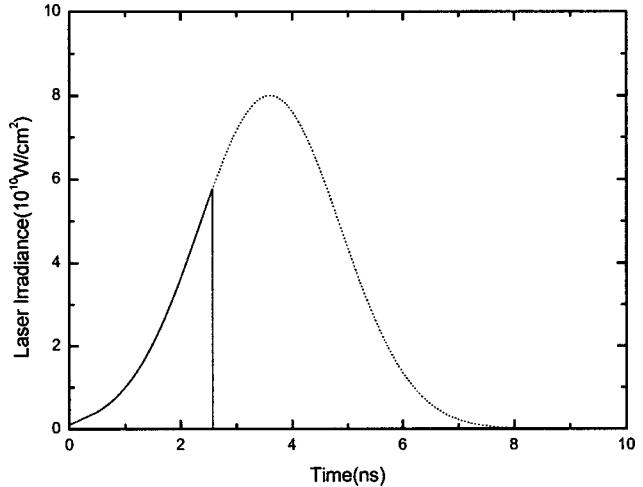
FIG. 4. The temporal profile of the laser irradiance reaching on the target surface for peak laser irradiance $I_0 = 8 \times 10^{10}$ W/cm^2. Solid line: with plasma shielding. Dotted line: without plasma shielding.

the trailing parts of the laser pulse are truncated (Fig. 4). This phenomenon has been verified by experiments in Ref. [16]. In this stage, the pressure of the plasma is much higher than that of the target surface. During the next 3-ns period, although the laser pulse is completed and no energy is provided, the pressure of the plasma is still higher than that of the target surface. In this third stage, the mass density of the target surface increases, but its temperature decreases. During the fourth stage, the plasma continues to expand and the number density and temperature of the plasma, as well as its pressure, decrease. The pressure is smaller than that at the target surface. The mass density of the target surface begins to decrease until it enters the unstable zone characterized by the occurrence of phase explosion.

In summary, we have developed a fluid model combined with the generalized van der Waals equation of state to describe the process of phase explosion during the interactions between a high-power nanosecond laser pulse and an Al target. The modeling results demonstrate that phase explosion does occur after the completion of the ablation laser pulse, which is consistent with recent experiments. Details of the phase explosion process are found to be related to the evolution of the laser-induced plasma. Although in our calculations the laser pulse is 3 ns and we choose Al as the target material, the mechanisms of phase explosion as revealed here should be applicable for a broad range of pulse durations as well as for other materials.

[1] *Laser Ablation and Deposition*, edited by J. C. Miller and R. F. Haglund (Academic, New York, 1998).

[2] A. Miotello and R. Kelly, Appl. Phys. Lett. **67**, 3535 (1995).

[3] K. Sokolowski-Tinten, J. Bialkowski, A. Cavalleri, D. Von der Linde, A. Oparin, J. Meyer-ter-Vehn, and S. I. Anisimov, Phys. Rev. Lett. **81**, 224 (1998).

[4] J. H. Yoo, S. H. Jeong, R. Greif, and R. E. Russo, J. Appl. Phys. **88**, 1638 (2000).

[5] J. H. Yoo, S. H. Jeong, X. L. Mao, R. Grief, and R. E. Russo, Appl. Phys. Lett. **76**, 783 (2000).

[6] R. C. Reid, Am. Sci. **64**, 146 (1976).

[7] M. M. Martynyuk, Sov. Phys. Tech. Phys. **19**, 793 (1974).

[8] M. M. Martynyuk, Sov. Phys. Tech. Phys. **21**, 430 (1976).

[9] Q. M. Lu, S. S. Mao, X. L. Mao, and R. E. Russo, Appl. Phys. Lett. **80**, 3072 (2002).

[10] F. Vidal, T. W. Johnston, S. Laville, O. Barthelemy, M. Chaker, B. Le Drogoff, J. Margot, and M. Sabsabi, Phys. Rev. Lett. **86**, 2573 (2001).

[11] M. M. Martynyuk, Russ. J. Phys. Chem. **57**, 810 (1983).

[12] A. Peterlongo, A. Miotello, and R. Kelly, Phys. Rev. E **50**, 4716 (1994).

[13] V. Yu Balandin, R. Niedrig, and O. Bostanjoglo, J. Appl. Phys. **77**, 135 (1995).

[14] J. G. Eberhart and H. C. Schnyders, J. Phys. Chem. **77**, 2730 (1973).

[15] R. J. Harrach, Lawrence Livermore Laboratory Report No. UCRL-52389, 1987 (unpublished).

[16] X. L. Mao and R. E. Russo, Appl. Phys. A: Mater. Sci. Process. **64**, 1 (1997).